A layered structure of bacterial and archaeal communities and their *in situ* activities in anaerobic granules

Running title: A layered structure in anaerobic granules

By

Hisashi Satoh, Yuki Miura, Ikuo Tsushima, and Satoshi Okabe*

Department of Urban and Environmental Engineering, Graduate school of Engineering, Hokkaido University, North-13, West-8, Sapporo 060-8628, Japan.

** Corresponding Author*

Satoshi OKABE

Department of Urban and Environmental Engineering, Graduate School of Engineering, Hokkaido University, North-13, West-8, Sapporo 060-8628, Japan.

Tel.: +81-(0)11-706-6266

Fax.: +81-(0)11-706-6266

E-mail: sokabe@eng.hokudai.ac.jp

ABSTRACT

The microbial community structure and spatial distribution of microorganisms and their *in situ* activities in anaerobic granules were investigated by 16S rRNA gene-based molecular techniques and microsensors for CH_4, H_2, pH, and oxidation-reduction potential (ORP). The 16S rRNA gene-cloning analysis revealed that the clones related to the phyla *Alphaproteobacteria* (detection frequency of 51%), *Firmicutes* (20%), *Chloroflexi* (9%), and *Betaproteobacteria* (8%) dominated the bacterial clone library and the predominant clones in the archaeal clone library were affiliated with *Methanosaeta* (73%). *In situ* hybridization with the oligonucleotide probes at the phylum level revealed that these microorganisms were numerically abundant in the granule. A layered structure of microorganisms was found in the granule, where *Chloroflexi* and *Betaproteobacteria* were present in the outer shell of the granule, *Firmicutes* was found in the middle layer, and aceticlastic *Archaea* was restricted to the inner layer. Microsensor measurements for CH_4, H_2, pH, and ORP revealed that acid and H_2 production occurred in the upper part of the granule, below which H_2 consumption and CH_4 production were detected. Direct comparison of the *in situ* activity distribution with the spatial distribution of the microorganisms implied that *Chloroflexi* contributed to degradation of complex organic compounds in the outermost layer, H_2 was produced mainly by *Firmicutes* in the middle layer, and *Methanosaeta* produced CH_4 in the inner layer. We could also determine the effective diffusion coefficient for H_2 in the anaerobic granules to be 2.66×10^{-5} cm^2 s^{-1}, which was 57% in water.

INTRODUCTION

The upflow anaerobic sludge blanket (UASB) reactors are commonly used in the treatment of high-strength municipal and industrial wastewaters. Their design permits the retention of a greater amount of active biomass (known as granules) in comparison with other anaerobic reactors. These anaerobic granules harbor several metabolic groups of microorganisms involved in the anaerobic degradation of complex organic compounds, including hydrolytic, fermentative, syntrophic, and methanogenic microorganisms. These different trophic groups of anaerobes closely and coordinately interact each other within the granules and convert complex organic compounds in wastewaters into methane (CH_4) and carbon dioxide (CO_2). The microbial communities of anaerobic granules treating different wastewaters have been investigated by culture-independent 16S rRNA gene-based molecular analyses (14, 22, 36), which allowed one to obtain more complete inventories of microorganisms in anaerobic granules. The results have shown that anaerobic granules consisted of a phylogenetically diverse group of microorganisms; however, the majority of them have not yet been cultivated (14, 22**,** 36).

The application of fluorescence *in situ* hybridization (FISH) with specific oligonucleotide probes further allows us to determine the abundance and *in situ* spatial distribution of specific phylogenetic groups in anaerobic granules (14, 20, 35, 41). By using the FISH technique, distinct multi-layered structures of different phylogenetic groups of microorganisms have been determined in different anaerobic granules cultivated on different substrates (20, 22, 35). These well-organized unique structures are thought to be a result of sequential degradation of complex organic compounds by each different trophic group within the granules, although it has not yet been confirmed experimentally.

In addition, spatial distribution of the microorganisms obtained from FISH analysis does not necessarily reflect microbial activity distributions. This is because the majority of microorganisms have not yet been cultivated, and phylogeny and phenotypes are not necessarily congruent with physiology. The spatial distributions of *in situ* metabolic functions in anaerobic granules have been poorly understood mainly due to a lack of specific analytical tools with a sufficient spatial resolution. Only a few studies have analyzed the distributions of glucose-degrading, fermentative, and sulfate-reducing activities in UASB granules by using microsensors for glucose, pH, and hydrogen sulfide (H_2S) (13, 21, 42). In these studies, CH_4 production rates were, however, not directly measured with microsensors. Santegoeds et al. (34) used CH_4 biosensors and H_2S microsensors to directly measure *in situ* methanogenic and sulfate-reducing activities in anaerobic granules, and then related them to the spatial distributions of methanogenic and sulfate-reducing bacterial populations. They demonstrated a distinct layered structure of microbial activities, in which sulfate reduction occurred in the outer layer, whereas CH_4 production was found in the center of the granules. However, they did not investigate the *in situ* distributions of fermentative and syntrophic populations and their activities in the granules, and hence the overall conversion mechanism of complex organic compounds to CH_4 within granules has not been elucidated.

To investigate the overall anaerobic conversion mechanism of organic compounds to CH_4 within anaerobic granules, we first analyzed the bacterial and archaeal community structures by 16S rRNA gene-cloning analysis, and then the spatial distribution of important phylogenetic groups in the granules was determined by fluorescence *in situ* hybridization (FISH). Second, we applied the microsensors for CH_4, H_2, pH, and oxidation-reduction

potential (ORP) to determine the spatial distribution of the *in situ* fermentative (H^+-producing), syntrophic (H_2-producing), and methanogenic activities in the granules. The microbial activity distribution was directly compared with the spatial distribution of the microorganisms.

MATERIALS AND METHODS

Sludge source.

Anaerobic granular sludge was collected from the bottom of a lab-scale upflow anaerobic sludge blanket (UASB) reactor (height, 50 cm; diameter, 5 cm) operated at 35°C. The reactor was inoculated with 0.7 liter of anaerobic granular sludge obtained from a full-scale UASB reactor treating the wastewater from an isomerized sugar-processing plant. The lab-scale reactor was fed with a synthetic medium at an average organic loading rate of 1.67 g chemical oxygen demand (COD) l^{-1} day^{-1} and a hydraulic residence time (HRT) of 8.2 h. The synthetic medium contained skim powdered milk (1,250 mg l^{-1}) as carbon and energy sources, $NaHCO_3$ (1,000 mg l^{-1}), K_2HPO_4 (50 mg l^{-1}), and the mineral solution (4). Granule samples were obtained from the lab-scale UASB reactor after 1 year of operation. The water qualities of the effluent during the sampling period were as follows (average ± standard deviation, n = 31): COD, 30 ± 9 mg l^{-1}; COD removal rate, 95 ± 1%; ORP, -230 ± 20 mV; gas production rate, 0.10 ± 0.02 liter h^{-1}; CH_4 content in gas, 55 ± 15%; CO_2 content in gas, 11 ± 4%; N_2 content in gas, 34 ± 17%; H_2 content in gas, 2300 ± 3300 ppm; acetate, 165 ± 81 μM; propionate, 77 ± 46 μM; and butyrate, 5.5 ± 7.7 μM. Other volatile fatty acids (butyrate, isobutyrate, and formate) were sometimes detected at trace levels.

DNA extraction and PCR amplification.

The granule samples were homogenized in the sterilized, distilled water and approximately 1.0-ml subsamples were subjected to DNA extraction. Total DNA was extracted from the homogenized granules with a FastDNA spin kit for soil (Bio 101; Qbiogene, Inc., Carlsbad, CA) as described in the manufacturer's instructions. 16S rRNA gene fragments were amplified from the extracted total DNA with *Taq* DNA polymerase (TaKaRa Bio, Inc., Ohtsu, Japan) by using a primer set of 11f (19) and 1492r (39) for bacterial community, and a primer set of A109f (40) and 1492r (39) for archaeal community. The PCR products were electrophoresed on a 1% (wt/vol) agarose gel and purified with a WIZARD PCR Preps DNA purification system (Promega). To reduce the possible PCR bias, the 16S rRNA gene was amplified in 6 to 10 PCR tubes and all tubes were combined for the next cloning step.

Cloning and sequencing of the 16S rRNA genes and phylogenetic analysis.

The purified PCR products were ligated into a qCR-XL-TOPO vector with a TOPO XL PCR cloning kit (Invitrogen, Carlsbad, CA). The ligated products were transformed into TOP10-competent *Escherichia coli* cells (Invitrogen). Plasmids were extracted from the cloned cells and purified with a Wizard Plus Minipreps DNA purification system (Promega). Nucleotide sequencing was performed with an automatic sequencer (3100 Avant genetic analyzer; Applied Biosystems). All sequences were checked for chimeric artifacts by using a CHECK_CHIMERA program from the Ribosomal Database Project (24). Partial sequences (approximately 500 bp) were compared with similar sequences of the reference organisms by a BLAST search (1). Sequences with 97% or greater similarity were grouped

into operational taxonomic units (OTUs) by a SIMILARITY_MATRIX program from the Ribosomal Database Project (24). Nearly complete sequencing of the 16S rRNA gene of each representative OTU was performed, and the sequences were aligned with a CLUSTAL W package (37). The Molecular Evolutionary Genetics Analysis (MEGA) program, version 3.1, was used to construct phylogenetic trees based on the neighbor-joining (33) and maximum-parsimony methods. Bootstrap resampling analysis of 1,000 replicates was performed to estimate the degree of confidence in tree topologies.

Fixation and cryosectioning of granule samples.

Granule samples were fixed in 4% paraformaldehyde solution for 8 h at 4°C, washed three times with phosphate-buffered saline (10 mM sodium phosphate buffer, 130 mM sodium chloride [pH 7.2]), and embedded in Tissue-Tek OCT compound (Sakura Finetek, Torrance, CA) overnight to infiltrate the OCT compound into the granule, as described previously (29). After rapid freezing at -21°C, 20-μm-thick slices were prepared with a cryostat (Reichert-Jung Cryocut 1800, Leica, Bensheim, Germany).

Fluorescent *in situ* hybridization.

In situ hybridization was performed according to the procedure described by Amann (2) and Okabe et al. (29). The following 16S and 23S rRNA-targeted oligonucleotide probes were used: EUB338 (3), EUB338 II (8), EUB338 III (8), ARC915 (31), ALF968 (28), BET42a (25), GNSB-941 (16), HGC69A (32), LGC354A (27), LGC354B (27), LGC354C (27), MB1174 (31), MG1200 (31), MS821 (31), and MX825 (31). The probes were labeled with fluorescein isothiocyanate (FITC) or tetramethylrhodamine 5-isothiocyanate (TRITC).

The phylum-specific probes were applied simultaneously with the ARC915 probe specific for *Archaea*. A model LSM510 confocal laser-scanning microscope (CLSM, Carl Zeiss, Oberkochen, Germany) equipped with an Ar ion laser (488 nm) and HeNe laser (543 nm) was used.

Microsensor measurements.

For microsensor measurements, the granules with ca. 2 mm in diameter were selected and positioned using five insect needles in the flow cell reactor (4.0 liter) that was filled with the synthetic medium used for the lab-scale UASB reactor at 35°C. The medium in the flow cell reactor was kept anaerobic by adding a reducing agent (thioglycolic acid at 100 mg l^{-1}) and by continuous bubbling with N_2, which also resulted in sufficient mixing of the medium. The ORP of the medium was ca. -200 mV. An average liquid velocity, judged from movement of suspended particles, was ca. 5 mm s^{-1}. The granules were acclimated in the medium for at least 6 h before measurement to ensure that steady-state profiles were obtained. The *in situ* steady-state concentration profiles of CH_4, H_2, pH, and ORP in the granules were measured using microsensors as described by Okabe et al. (30). At least three concentration profiles were measured for each chemical species. For practical reasons, a concentration profile was measured only once in a granule, therefore, concentration profiles of different chemical species were measured in different granules.

Microscale biosensors for CH_4 were constructed as described by Damgaard and Revsbech (11). Because all measurements were performed under anoxic conditions, an oxygen-scavenging guard capillary (12) was not applied. Hence, the CH_4 microsensor was assembled from an oxygen microsensor, a gas capillary, and a medium capillary. The tip

diameters of the microsensors were 50-100 μm. A culture of the methane-oxidizing bacterium, *Methylosinus trichosporium* (ATCC 49243), was injected into the medium capillary. The principle of the CH_4 microsensor is based on a counter diffusion of oxygen and CH_4. CH_4 diffusing through the membrane of the medium capillary is consumed by the the methane-oxidizing bacteria with a concomitant decrease of oxygen inside the reaction space (i.e., the medium capillary). Oxygen consumed is detected by the internal oxygen microsensor and translated into a CH_4 partial pressure by calibration. Calibration was routinely performed before and after a measurement by placing a CH_4 microsensor in a calibration chamber (100 ml) into which CH_4 and N_2 gases were continuously blown at known flow rates at 35°C. After the sensor signal stabilized, the signal was monitored and the CH_4 concentration was measured by a gas chromatography. CH_4 concentration was changed stepwise by changing the flow rates of CH_4 and N_2 gases. This procedure was repeated over the full range of 0 to 100% CH_4 saturation. The response to 0% CH_4 saturation (i.e., 100% N_2 saturation) was typically between 70 and 90 pA, and 90% response times were ca. 200 s. The response was linear ($r^2 > 0.95$) over the range of 0 to 100% CH_4 saturation. The slope of the calibration carves was ca. 20 pA per atm of CH_4 (see **Fig. S1** in the supplemental material). Sensor life span was ca. 2 weeks. If the slope of the calibration curve was less than 10 pA per atm of CH_4, the microsensor was discarded.

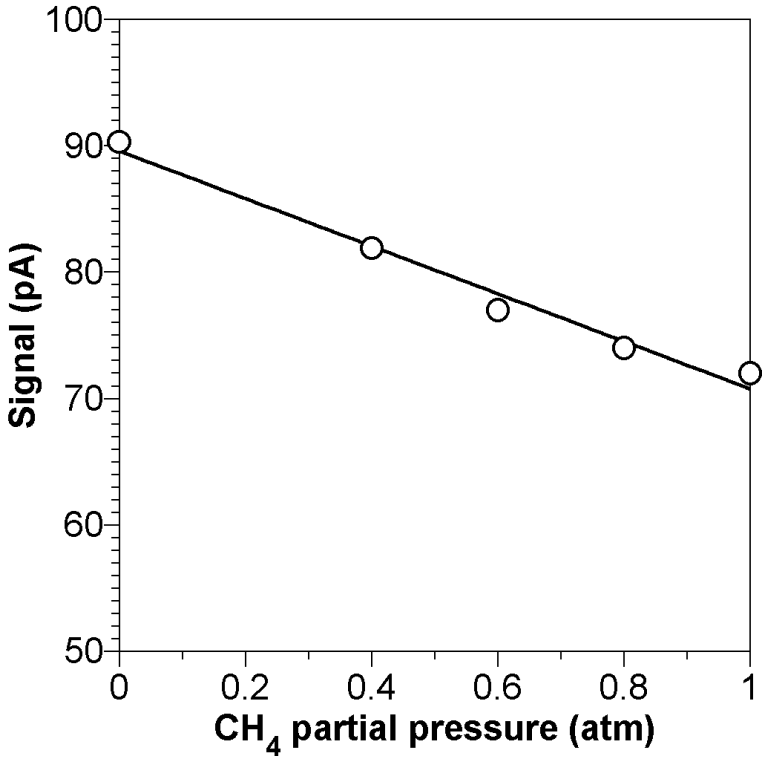

Fig. S1. A typical calibration curve for a microscale biosensor for methane. The solid line indicates linear regression. The equation of the straight line was $y = -19 x + 90$ with $r^2 = 0.98$.

Polarographic H_2 microsensors were constructed as described by Ebert and Brune (15). The tip diameters of the microsensors were ca. 10 μm, 90% response times were less than 2 s, and the detection limit was ca. 1 μM. Calibration was routinely performed by immersing a microsensor in a calibration chamber filled with the synthetic medium which continuously bubbled with H_2 and N_2 gases. The H_2 concentration in the medium was measured by a gas chromatography. H_2 concentration was changed stepwise by changing the flow rates of H_2 and N_2 gases. ORP microsensors, which were made from a platinum wire coated with a glass micropipette, were constructed and calibrated as described by Jang et al. (18). All ORP data reported in this paper were the potential difference measured between an ORP microsensor

and the Ag/AgCl reference electrode. Potentiometric pH microsensors were constructed, calibrated, and used according to the protocol as described by Okabe et al. (29).

Microbial activity calculations.

Net volumetric CH_4 and H_2 production rates ($R(CH_4)$ and $R(H_2)$, respectively) in the granule were estimated from the steady-state concentration profiles of CH_4 and H_2 by using Fick's second law of diffusion as previously described by Santegoeds et al. (34) and Lorenzen et al. (23). Furthermore, the total H_2 production rate from the granule was calculated using Fick's first law of diffusion (29). Molecular diffusion coefficients ($D_{w\,25}$) of 1.49×10^{-5} cm^2 s^{-1} for CH_4 and 4.50×10^{-5} cm^2 s^{-1} for H_2 in water at 25°C were used for the calculations (7). Molecular diffusion coefficients in water at 35°C ($D_{w\,35}$) were calculated according to the Stokes-Einstein relationship (7). Furthermore, effective diffusion coefficient (D_{eff}) of these compounds in the granules were estimated by correcting D_w with the ratio of the diffusivities in granules and in water (57%), as determined with the H_2 microsensor in this study (see Discussion).

Estimation of effective diffusion coefficient (D_{eff}).

Granules with a diameter of ca. 2 mm were selected and deactivated in pure chloroform for 10 min. After being rinsed, the deactivated granule was mounted in the flow cell reactor containing the synthetic medium for microsensor measurements at 35°C, and a H_2 microsensor was positioned in the center of the granule with a micromanipulator. After preincubation for at least 30 min, H_2 gas was bubbled. The evolution of the H_2 concentration in the center of the granule was monitored over time in triplicate, and the average D_{eff} was

calculated according to the protocol as described by Cronenberg and van den Heuvel (6).

Chemical analyses.

The concentrations of chemical oxygen demand (COD) were determined according to the standard methods (5). Volatile fatty acids were determined by high-performance liquid chromatography (LC-10AD system; Shimadzu Co., Kyoto, Japan) equipped with a Shimadzu Shim-pack SCR-102H column (0.8 by 30 cm) after filtration with 0.2-μm-pore size membranes (Advantec Co., Ltd., Tokyo, Japan). CH_4, H_2, and CO_2 in gaseous samples were determined by gas chromatography (GC-14B; Shimadzu Co., Kyoto, Japan) equipped with a thermal-conductivity detector and a Shincarbon-ST column (Shimadzu Co., Kyoto, Japan). ORP and pH were directly determined using an ORP and a pH electrode, respectively.

Nucleotide sequence accession numbers.

The GenBank/EMBL/DDBJ accession numbers for the 16S rRNA gene sequences of the clones used for the phylogenetic analysis are AB329636 to AB329664.

Results

Bacterial and archaeal community structures.

16S rRNA gene clone libraries of *Bacteria* and *Archaea* were constructed from the anaerobic granule samples taken from the UASB reactor. From the *Bacteria* clone library 105 clones were randomly selected and the partial sequences of about 500 bp were analyzed. In total, the clones were grouped into 25 OTUs on the basis of more than 97% sequence similarity within an OTU. Then, a nearly complete 16S rRNA gene sequence of a representative clone of each OTU was analyzed. The phylogenetic trees were constructed by neighbor-joining and maximum-parsimony methods, and both methods resulted in essentially the same topology. The phylogenetic tree inferred by the neighbor-joining method is shown in **Fig. 1**. The distribution of cloned sequences among phyla is as follows: *Alphaproteobacteria*, 51%; *Firmicutes*, 20%; *Chloroflexi*, 9%; *Betaproteobacteria*, 8%; *Actinobacteria*, 4%; *Deltaproteobacteria*, 3%; *Cyanobacteria*, 2%; *Gammaproteobacteria*, 2%; *Epsilonproteobacteria*, 1%; and *Bacteroidetes*, 1%. The most frequently detected clones (40 of 105 clones) were represented by OTU 8, which was closely related to the *Sphingomonas rhizogenes* (99.8% sequence similarity).

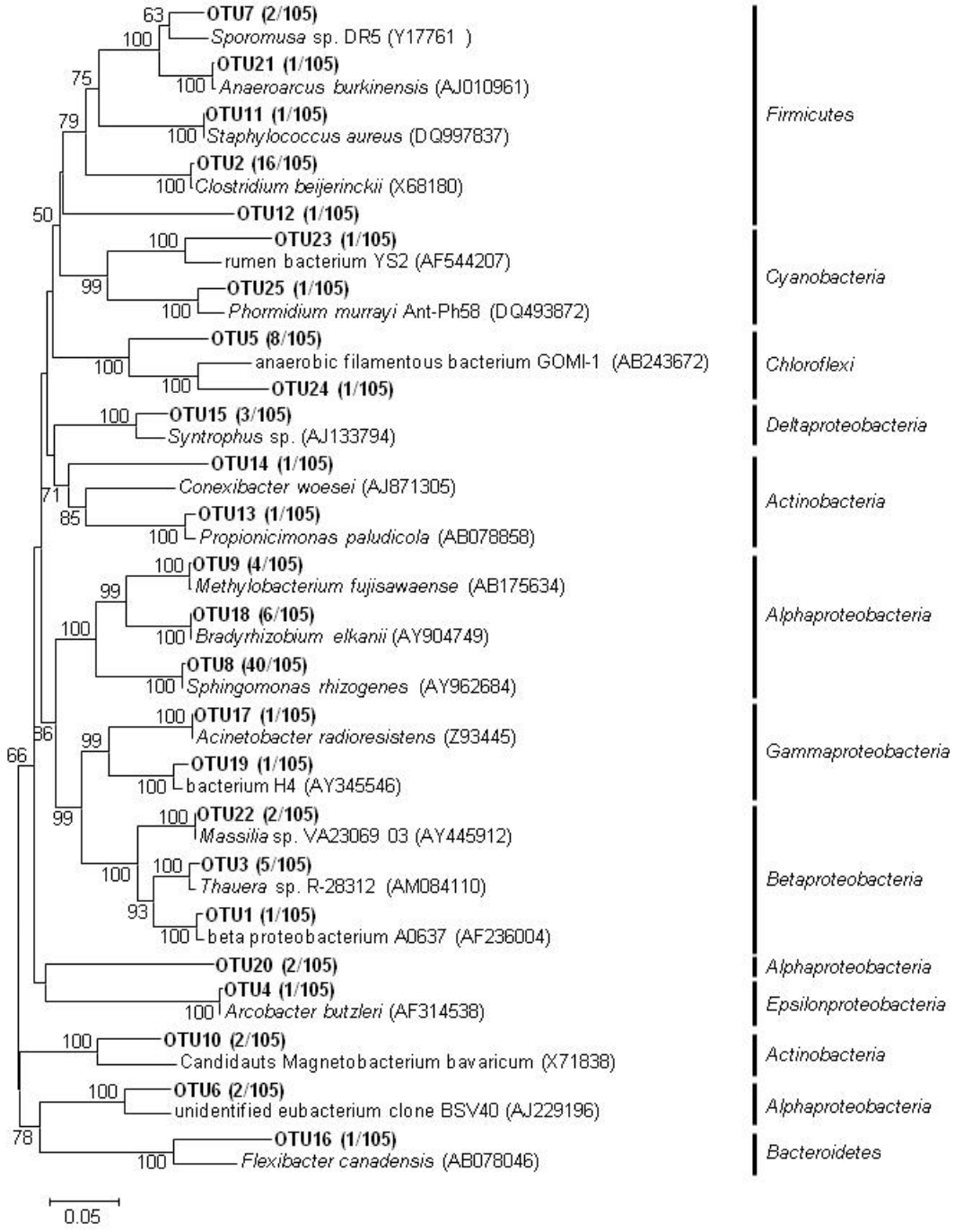

Fig. 1. Phylogenetic tree representing the affiliation of the 16S rRNA clone sequences of *Bacteria* retrieved from granule samples (OTU#). The tree was generated by using nearly full length of 16S rRNA gene sequences and the neighbor-joining method. The scale bar represents 5% estimated divergence. The numbers at the nodes are bootstrap values (1,000 replicates) with more than 50% bootstrap support.

For the *Archaea* clone library, 48 clones were randomly selected and partial sequences of about 500 bp were analyzed. The clones were grouped into 4 OTUs. The clones belonging to OTUs 1 and 4 were related to *Methanosaeta* whereas the clones belonging to the other OTUs (OTUs 2 and 3) were related to *Methanomicrobiales*. Their representative sequences were used for phylogenetic analysis (**Fig. 2**). The most frequently detected clones (33 of 48, detection frequency of 69%) represented by OTU 1 were affiliated with *Methanosaeta concilii* with 98.3% sequence similarity. The clones represented by OTU 4 (2 of 48, detection frequency of 4%) were affiliated with *Methanosaeta harundinacea* with 99.6% sequence similarity. The clones represented by OTU 2 (9 of 48, detection frequency of 19%) and OTU 3 (4 of 48, detection frequency of 8%) were related to the orders *Methanomicrobiales* with 96.2% and 97.8% sequence similarities, respectively. These results indicated that diversity of the *Archaea* clone library was lower than for the *Bacteria*.

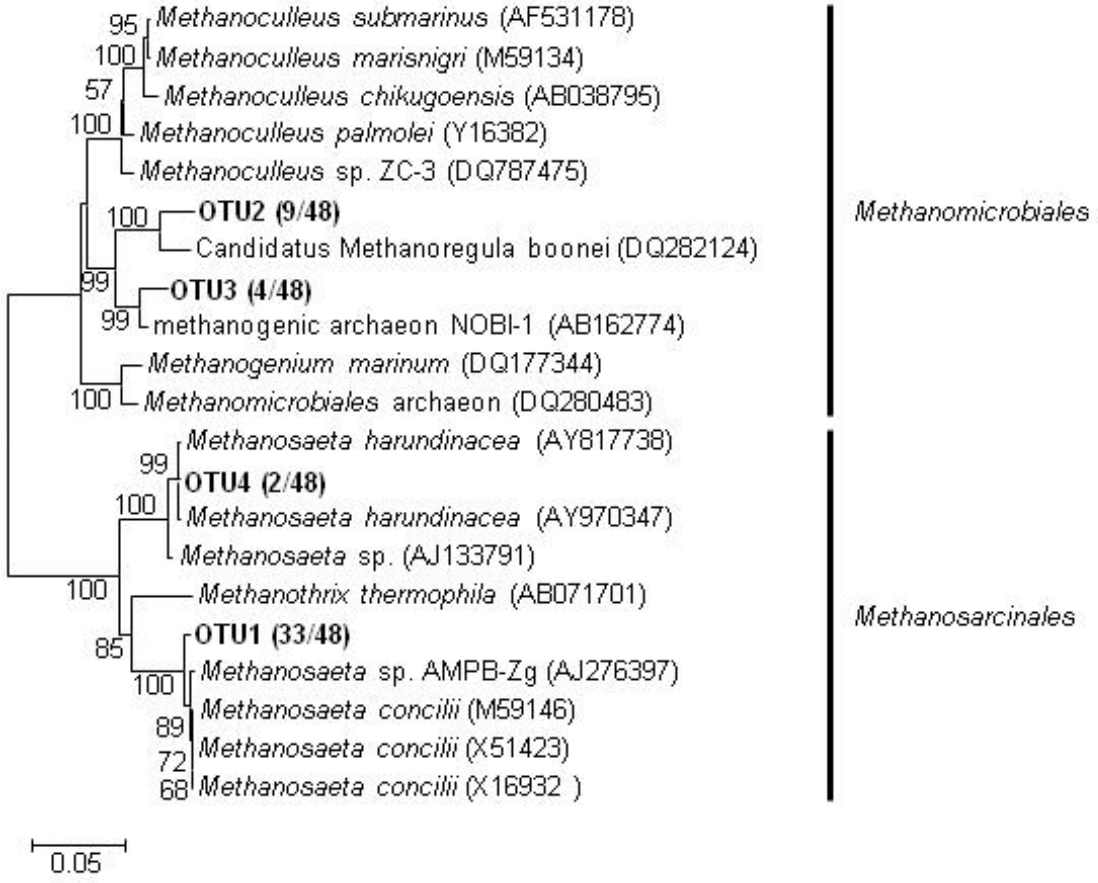

Fig. 2. Phylogenetic tree representing the affiliation of the 16S rRNA clone sequences of *Archaea* retrieved from granule samples (OTU#). The tree was generated by using nearly full length of 16S rRNA gene sequences and the neighbor-joining method. The scale bar represents 5% estimated divergence. The numbers at the nodes are bootstrap values (1,000 replicates) with more than 50% bootstrap support.

Spatial distribution of microorganisms in granules.

Cross-sectional differential interference contrast (DIC) images of the granule showed that the granule had a multi-layered structure consisting of biomass and interstitial voids (**Fig. 3A**). Analysis of the granule after staining with DAPI showed microorganisms were predominantly present in the outer 400 μm (**Fig. 3A**). It is most likely that the dark

nonstaining center consisted of inert matter and dormant microbial cells. This is probably attributed to substrate limitation in the center of the granules due to the relatively low COD loading rate in the reactor analyzed. The nonstaining center was always observed in the granules analyzed with diameters exceeding about 1,000 μm. FISH using FITC-labeled EUB338-mixed probe and TRITC-labeled ARC915 probe revealed that the outer layer (ca. 250-μm-thick) was dominated by bacterial cells whereas the inner layer (below 250 μm from the surface) was occupied mainly by archaeal cells (**Fig. 3B**). Archaeal and bacterial signals were low in the granule interior (below ca. 400 μm from the surface). This layered structure was repeatedly observed in all of the granular sections analyzed. Filamentous cells were observed in the uppermost layer of the granules and these cells were hybridized with the probe GNSB-941 specific for almost all members of the phylum *Chloroflexi* (**Fig. 3C**). The BET42a-stained cells were also present in the outer shell of the granule (**Fig. 3D**). The cells hybridized with the probe LGC354 specific for *Firmicutes* were numerically most abundant *Bacteria* in the inner layer of the granule (**Fig. 3E**). The abundance and fluorescent intensity of ALF968-stained cells were low (**Fig. 3F**) although the bacterial clone library was predominated by the members of *Alphaproteobacteria* (**Fig. 1**). The MX825-stained cells surrounded the dense spherical microcolonies that composed of a number of coccoid cells stained with the probe HGC69A (i.e., *Actinobacteria*) in the middle layer (at a depth of ca. 200 μm) of the granules (**Fig. 3G**). Among archaeal cells, the MX825-stained cells (i.e., *Methanosaeta*) predominated while the remaining portion of archaeal cells could not be hybridized with the MG1200, MB1174, and MS821 probes (data not shown).

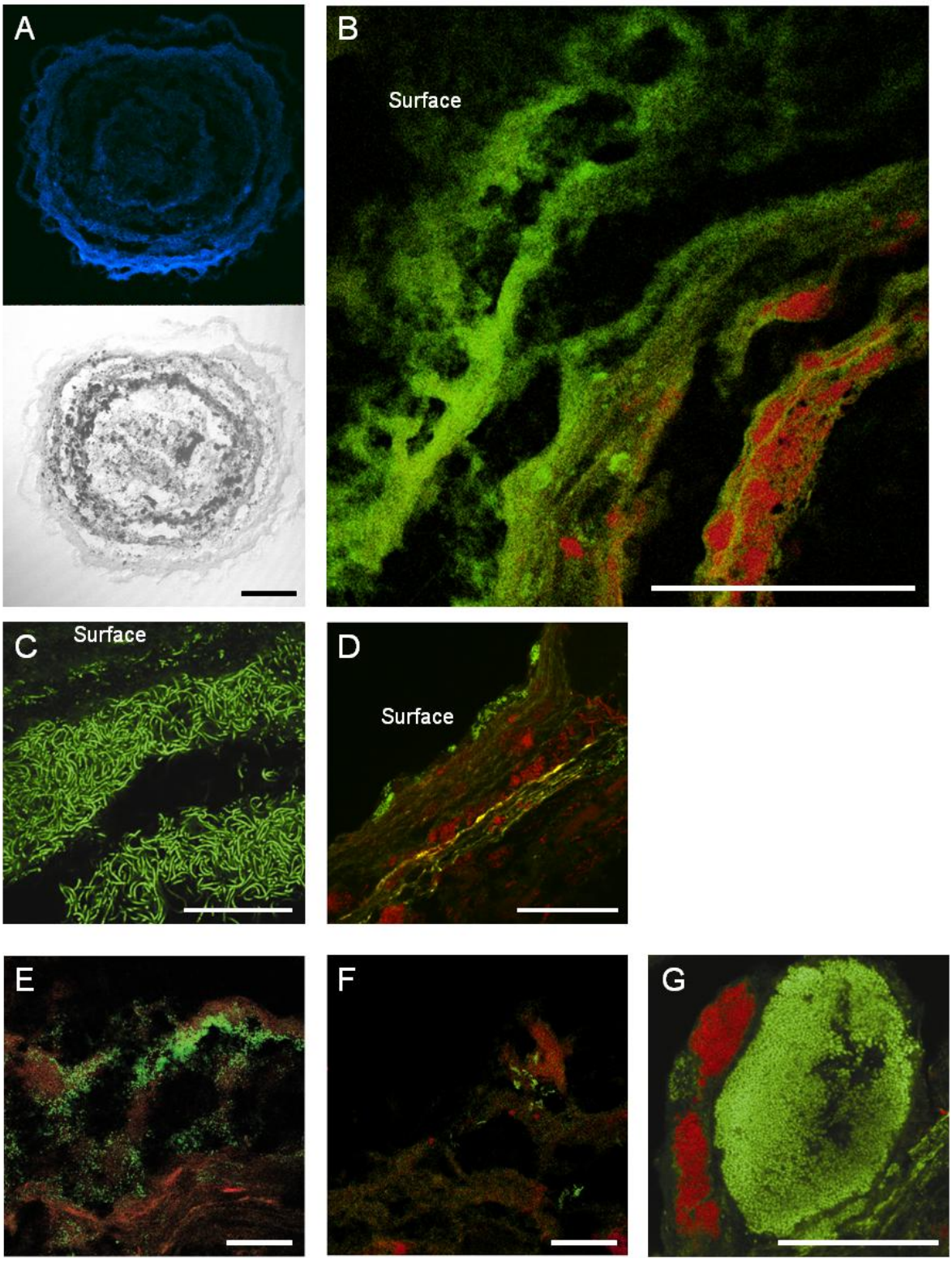

Fig. 3 Confocal laser scanning microscope images of thin sections of the anaerobic granules showing the *in situ* spatial organization of bacteria and archaea. (A) Staining with DAPI and differential interference contrast (DIC) image. (B) FISH with TRITC-labeled probe

ARC915 (red) and FITC-labeled EUB338-mixed probe (green). (C) FISH with FITC-labeled probe GNSB-941. (D) FISH with TRITC-labeled probe ARC915 (red) and FITC-labeled probe BET42a (green). (E) FISH with TRITC-labeled probe ARC915 (red) and FITC-labeled probe LGC354 (green). (F) FISH with TRITC-labeled probe ARC915 (red) and FITC-labeled probe ALF968 (green). (G) FISH with TRITC-labeled probe MX825 (red) and FITC-labeled probe HGC69A (green). Scale bars indicate 200 μm (A, B) and 50 μm (C-G).

Concentration profiles and spatial distribution of microbial activities.

Steady-state concentration profiles of ORP, pH, H_2, and CH_4 in the granules are shown in **Fig. 4**. pH decrease (i.e., acid production) was found in the upper part of the granule and below which pH increased (**Fig. 4A**). When H_2 profiles were measured in the medium without $NaHCO_3$, H_2 profile showed a peak of 26 μM at a depth of 100 μm and H_2 concentration readily decreased in the inner layer of the granule (**Fig. 4B**). The addition of 12 mM of $NaHCO_3$ stimulated H_2 consumption activity and H_2 concentration in the granule became under detection limit (1 μM) (data not shown). CH_4 concentration gradually increased throughout the granule and its gradient was steeper in the outer layer of the granule (**Fig. 4B**).

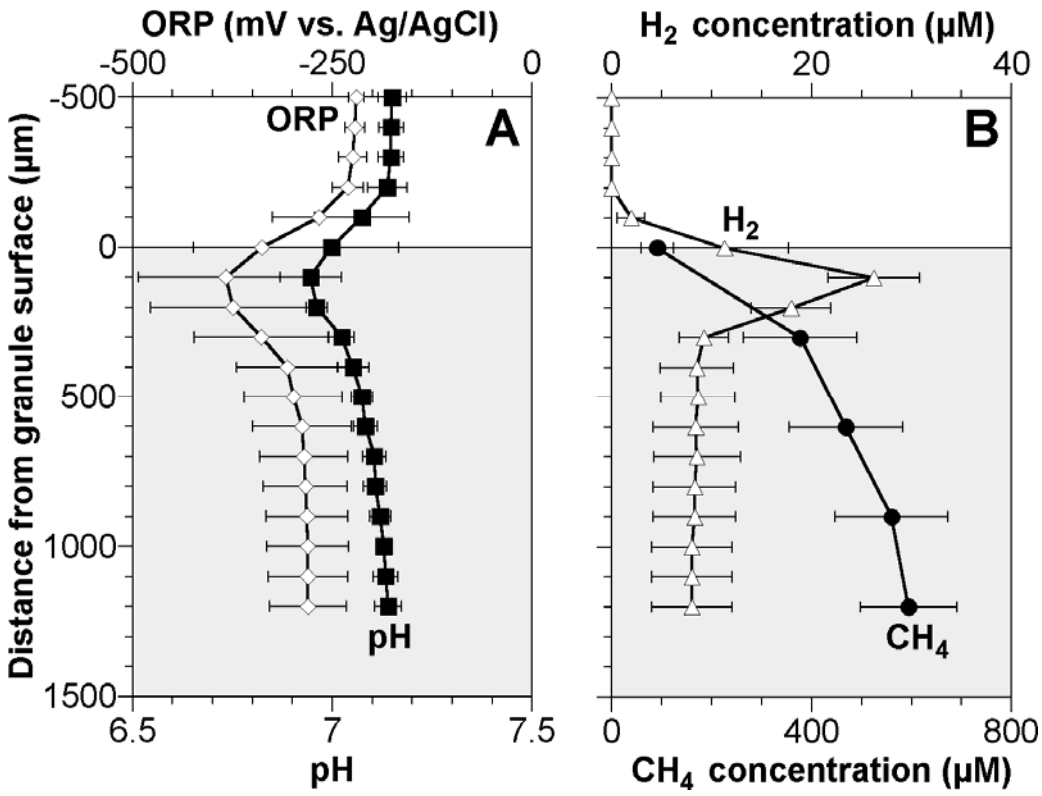

Fig. 4. Concentration profiles of pH, ORP, CH_4 and H_2 in the anaerobic granule. The profiles are average values (n = 3) and error bars represent the standard deviations of triplicate measurements. Zero on the vertical axis corresponds to the surface of the granule.

The spatial distributions of $R(CH_4)$ and $R(H_2)$ were calculated on the basis of the measured profiles. **Fig. 5** shows that anaerobic processes occurred in distinctly different layers within the granule. H_2 production was exclusively detected at a depth of 100 μm. H_2 produced was partly consumed below 300 μm from the surface and emitted from the granule with the total production rate of 2.3 ± 4.3 μmol cm^{-2} h^{-1}. CH_4 was produced mainly in the inner layer (below ca. 300 μm from the surface) with the maximum rate of 11.5 ± 3.9 μmol

cm^{-3} h^{-1} at a depth of 300 μm.

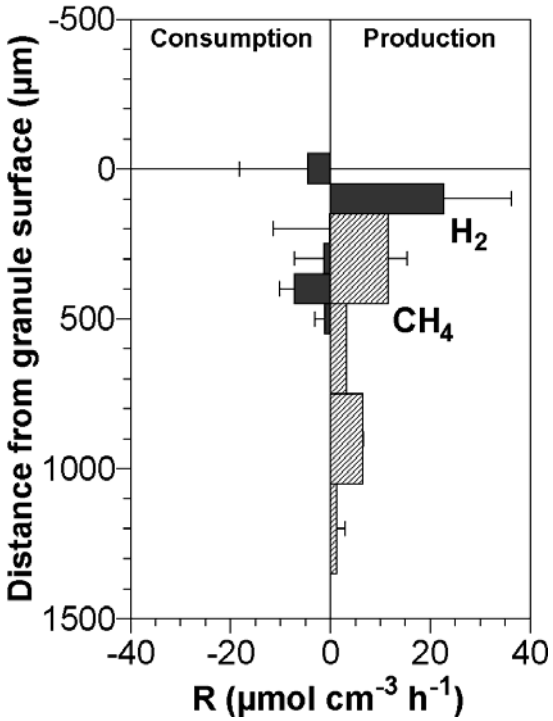

Fig. 5. Spatial distribution and magnitude of the net volumetric production rates of CH_4 and H_2. The rates were calculated based on the corresponding concentration profiles shown in **Fig. 4**. The profiles are average values (n = 3) and error bars represent the standard deviations of triplicate measurements. Negative values indicate consumption rates. Zero on the vertical axis corresponds to the surface of the granule.

Transient measurements for determination of effective diffusion coefficient (D_{eff})

For the determination of D_{eff}, continuous monitoring of H_2 concentrations at the center of the granule deactivated by pure chloroform was performed. The ratio of H_2 concentration at the granule center to one in the bulk liquid (C/C_b) was calculated, and a representative profile of C/C_b transient is shown in **Fig. 6**. A mathematical model that describes the C/C_b transient in the granule provided a good fit to the profile measured (correlation coefficient

of 0.98). Based on the model, D_{eff} for H_2 in the granules were determined to be 2.66 ± 0.13 × 10^{-5} cm^2 s^{-1} (average ± standard deviation, n = 3).

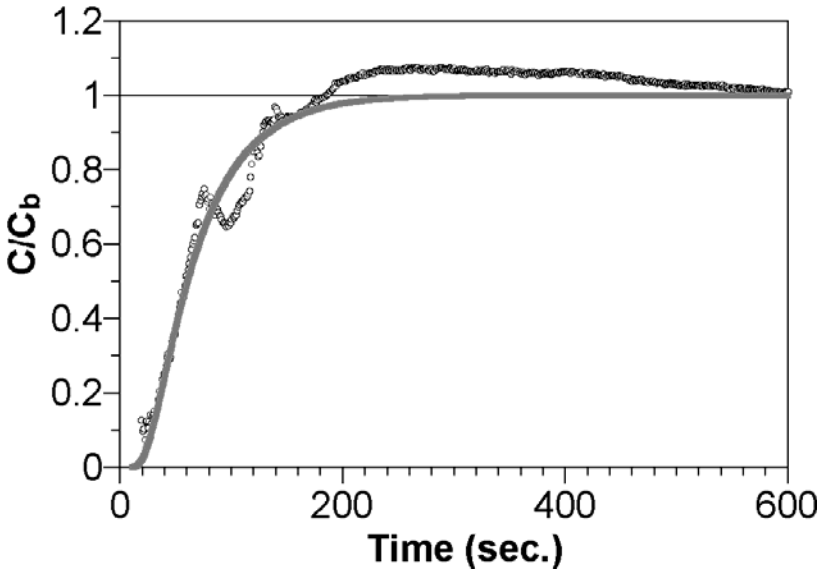

Fig. 6. A typical transient H_2 concentration profile measured at the center of the granule inhibited by chloroform. Points indicate H_2 concentrations measured and a solid line is a theoretical curve.

Discussion

The microsensor measurements indicated a distinct layered structure of the microbial activities in the anaerobic granule, with net acid (H^+) and H_2 production (i.e., fermentative and syntrophic activities) at a depth of 100 μm, and net H_2 consumption and CH_4 production (i.e., methanogenesis) below 300 μm from the surface (**Fig. 5**). Because anaerobic degradation of organic compounds is a multi-step process, a layered structure of the bacteria that hydrolyze complex organic compounds in wastewater to fundamental structural building blocks (e.g., glucose and amino acids) at the granule surface, fermentative bacteria that ferment these products to fatty acids and subsequently syntrophic bacteria oxidizing

fatty acids and alcohols to H_2 and acetate in the middle layer, and methane-producing archaea in the inner layer, was developed. Our knowledge of the spatial distribution of microbial activities, especially CH_4-producing activity in anaerobic granules is very limited because *in situ* activity measurements require specific analytical tools (e.g., microsensors). CH_4 microprofiles and the distributions of CH_4 production activity in a sewage biofilm (10), a rice paddy soil (12), and a lake sediment (9) have been measured with micrometer resolution by using CH_4 microsensors. Only one study indicated CH_4 microprofiles in anaerobic granules (34). This study demonstrated a similar layered structure of the microbial activities in methanogenic-sulfidogenic aggregates in which sulfidogenic activity was found in the outer layer and CH_4 production only started from 300 μm onwards inside the aggregate. In our study, although a sulfate reduction zone was not analyzed, sulfate reduction rate could be very low because sulfate concentration was less than 2 μM in the synthetic medium for cultivation and microsensor measurements.

In situ hybridization results showed that the outer layer (ca. 250-μm-thick) of the granule was dominated by *Bacteria* whereas the inner layer (below 250 μm from the surface) consisted of *Archaea* (**Fig. 3B**). Similar layered structures of microorganisms in anaerobic granules have been reported elsewhere (20, 35). Direct comparison of the microsensor results with the FISH ones revealed that H_2 might be produced at a depth of 100 μm mainly by members of *Firmicutes*, and *Archaea* affiliated with *Methanosaeta* produced CH_4 below 300 μm. Phylogenetic analysis revealed that members of the phyla *Alphaproteobacteria*, *Firmicutes*, *Chloroflexi*, and *Betaproteobacteria* dominated the bacterial clone library. This result was in good agreement with the FISH ones. *Chloroflexi* was mainly detected in the granule surface (**Fig. 3C**), indicating that they contributed to the

hydrolysis of complex organic compounds. Ariesyady et al. (4) analyzed *in situ* function (i.e., glucose-, propionate-, butyrate-, and acetate-degrading activities) of bacteria in a full-scale anaerobic sludge digester by microautoradiography (MAR)-FISH technique, and revealed that *Chloroflexi* was one of the numerically dominant glucose-degrading bacterial groups. The filamentous *Chloroflexi*-like bacteria also contributed to coating of other microorganisms and formation of dense and compact granules. The bacteria belonging to *Firmicutes* have been detected in methanogenic granules (14, 22). These bacteria can anaerobically utilize glucose, propionate, butyrate, and acetate (4), and produce H_2 (17). In contrast, Ariesyady et al. (4) demonstrated that glucose-utilizing rate of *Betaproteobacteria* was very low and *Alphaproteobacteria* did not utilize all of the substrates tested (i.e., glucose, propionate, butyrate, and acetate) in an anaerobic sludge digester, indicating less contribution of these bacteria to the degradation of organic compounds in the granules.

The clones affiliated with aceticlastic *Methanosaeta* were frequently detected in the archaeal clone library (**Fig. 2**), and the cells hybridized with the probe MX825 specific for the genus *Methanosaeta* were the dominant member of *Archaea* in the granule. In general, aceticlastic methanogens are more abundant than hydrogenotrophic ones in methanogenic consortia (14, 35). Although the hydrogenotrophic methanogens affiliated with *Methanomicrobiales* were identified by phylogenetic analysis, the number of hydrogenotrophic methanogens hybridized with probes MG1200 and MB1174 was under detection limit in this study. The probe MG1200 is specific for *Methanomicrobiales* whereas the probe MB1174 is specific for *Methanobacteriales*. Moreover, the 16S rRNA gene sequence of the clones belonging to OTU2 in the *Archaea* clone library, which were more frequently detected than those belonging to OTU3, had two mismatches with the probe

MG1200 sequence. Therefore, further studies are urgently needed to identify the hydrogenotrophic methanogens with additional oligonucleotide probes for hydrogenotrophic methanogens, and evaluate the significance of them in methane production.

We could determine the effective diffusion coefficient (D_{eff}) for H_2 in the anaerobic granules with H_2 microsensors. In this study, D_{eff} for H_2 in the granules at 35°C was 2.66 ± 0.13 × 10^{-5} cm^2 s^{-1}, which was 57 ± 3% of the molecular diffusion coefficient for H_2 in water ($D_{w\,35}$; 4.65 × 10^{-5} cm^2 s^{-1}). The similar ratios were reported for glucose by applying microsensors to anaerobic granules (21, 34). Based on the results, the D_{eff} for CH_4 and H_2 were assumed to be 57% of their D in water, and these values were used to calculate the microbial activities (R) in the granules (**Fig. 5**). The calculated CH_4 production rates in the granule (11.5 μmol cm^{-3} h^{-1}) were comparable to those in the methanogenic aggregates (ca. 15 μmol cm^{-3} h^{-1}) (34) and were two orders of magnitude higher than those in a sewage biofilm (ca. 0.18 μmol cm^{-3} h^{-1}) (10). High CH_4 production activity of the anaerobic granules might be attributed to higher abundance of methanogens.

Maximum H_2 concentration (26 μM) in the granule (**Fig. 4B**) was one order of magnitude higher than that in anaerobic aggregates (less than 5 μM) (34). In contrast, these values were lower than those in the hindgut of a wood-feeding lower termite (ca. 50 μM) (15). In methanogenic consortia, H_2 produced by syntrophic bacteria should be efficiently consumed because the oxidation of intermediary metabolites (e.g., fatty acids and alcohols) into H_2 is thermodynamically feasible only at very low H_2 partial pressures (e.g., between 10^{-4} and 10^{-6} atm for anaerobic propionate degradation) (26). To investigate whether H_2 concentrations in the granule analyzed in this study were low enough to carry out the

syntrophic H_2-producing reaction (e.g., propionate oxidation), the relationship between H_2 concentration and the Gibbs free energy change (ΔG) for propionate oxidation was calculated according to the following equation (38).

$$\Delta G = \Delta G_0' + RT \ln ([H_2]^3 [Ace] / [Pro])$$

where ΔG is the actual free energy, $\Delta G_0'$ is the standard free energy (76.5 kJ mol^{-1}), R is the ideal gas constant, T is the temperature (K), and $[H_2]$, [Ace], and [Pro] are the molar H_2, acetate, and propionate concentrations, respectively. The average concentrations of propionate (77 μM) and acetate (165 μM), and temperature (35°C) in the lab-scale UASB reactor analyzed were used for the calculation. The H_2 concentration for ΔG = 0 was calculated to be 36.8 μM, indicating that the H_2 concentration in the granule (< 26 μM) was low enough for the syntrophic degradation to proceed.

There was a difficulty with microsensor measurements. It was curious that low but significant CH_4-producing activities were detected in the center of the granule in which the density of *Archaea* was low. A possible explanation could be compression of the granule by inserting the CH_4 microsensor, because its tip diameter was relatively large (50-100 μm) and conical as compared with those of other microsensors. Therefore, CH_4 concentration profiles were monitored by advancing the microsensor in steps of 300 μm (**Fig. 4B**).

In conclusion, combining the 16S rRNA gene-based molecular techniques with microsensors provided direct information about phylogenetic diversities, spatial distributions, and activities of *Bacteria* and *Archaea* in anaerobic granules. The spatial distributions of the microorganisms and their *in situ* activities in the granule were characterized by a distinct layered structure. Acid and H_2 production occurred in the upper part of the granule, below which H_2 consumption and CH_4 production were found.

Chloroflexi might contribute to the hydrolysis of complex organic compounds in the outer shell of the granule, H_2 was produced mainly by members of *Firmicutes* in the middle layer, and *Archaea* affiliated with *Methanosaeta* produced CH_4 in the inner layer. Further studies with the microsensor for volatile fatty acids and additional oligonucleotide probes for syntrophic bacteria and hydrogenotrophic methanogens are needed for better understanding of the overall degradation mechanism of complex organic matter in anaerobic granules.

Acknowledgement

This study was carried out as a part of "The Project for Development of Technologies for Analyzing and Controlling the Mechanism of Biodegrading and Processing" which was entrusted by the New Energy and Industrial Technology Development Organization (NEDO), Japan. This work was partially supported by a grant-in-aid (18710013) for developmental scientific research from the Ministry of Education, Science and Culture of Japan, and by funding from the Maeda Engineering Foundation. We thank Tsukasa Ito and Tomonori Kindaichi for valuable assistance and discussions during preparation of the manuscript.

References

1. **Altschul, S. F., T. L. Madden, A. A. Schaffer, J. Zhang, Z. Zhang, W. Miller, and D. J. Lipman.** 1997. Gapped BLAST and PSI-BLAST: a new generation of protein database search programs. Nucleic Acids Res. 25:3389–3402.
2. **Amann, R. I.** 1995. In situ identification of microorganisms by whole cell hybridization with rRNA-targeted nucleic acid probes, p. 1–15. *In* A. D. L. Akkerman,

J. D. van Elsas, and F. J. de Bruijn (ed.), Molecular microbial ecology manual. Kluwer Academic Publishers, Dordrecht, The Netherlands.

3. **Amann, R. I., B. J. Binder, R. J. Olson, S. W Chisholm, R. Devereux, and D. A. Stahl.** 1990. Combination of 16S rRNA-targeted oligonucleotide probes with flow cytometry for analyzing mixed microbial populations. Appl. Environ. Microbiol. **56:**1919–1925.

4. **Ariesyady, H. D., T. Ito, and S. Okabe.** 2007. Functional bacterial and archaeal community structures of major trophic groups in a full-scale anaerobic sludge digester. Water Res. **41:**1554–1568.

5. **Clesceri, L., A. Greenberg, and A. Eaton (ed.).** 1998. Standard methods for the examination of water and wastewater. American Public Health Association, Washington, D.C.

6. **Cronenberg, C., and J. C. van den Heuvel.** 1991. Determination of glucose diffusion coefficients in biofilms with microsensors. Biosens. Bioelectronics **6:**255–262.

7. **Cussler, E. L**. 1997. Diffusion mass transfer in fluid systems, 2nd ed. Cambridge University Press, Cambridge, England.

8. **Daims, H., A. Brühl, R. Amann, K.-H. Schleifer, and M. Wagner.** 1999. The domain-specific probe EUB338 is insufficient for the detection of all bacteria: development and evaluation of a more comprehensive probe set. Syst. Appl. Microbiol. **22:**434–444.

9. **Damgaard, L. R., L. H. Larsen, and N. P. Revsbech.** 1995. Microscale biosensors for environmental monitoring. Trends Anal. Chem. **14:**300–303.

10. **Damgaard, L. R., L. P. Nielsen, N. P. Revsbech.** 2001. Methane microprofiles in a

sewage biofilm determined with a microscale biosensor. Water Res. **35:**1379–1386.

11. **Damgaard, L. R., and N. P. Revsbech.** 1997. A microscale biosensor for methane containing methanotrophic bacteria and an internal oxygen reservoir. Anal. Chem. **69:**2262–2267.
12. **Damgaard, L. R., N. P. Revsbech, and W. Reichardt.** 1998. Use of an oxygen-insensitive microscale biosensor for methane to measure methane concentration profiles in a rice paddy. Appl. Environ. Microbiol. **64:**864–870.
13. **de Beer, D., J. W. Huisman, J. C. Van den Heuvel, and S. P. P. Ottengraf.** 1992. The effect of pH profiles in methanogenic aggregates on the kinetics of acetate conversion. Water Res. **26:**1329–1336.
14. **Díaz, E. E., A. J. M. Stams, R. Amils, and J. L. Sanz.** 2006. Phenotypic properties and microbial diversity of methanogenic granules from a full-scale upflow anaerobic sludge bed reactor treating brewery wastewater. Appl. Environ. Microbiol. **72:**4942–4949.
15. **Ebert, A., and A. Brune.** 1997. Hydrogen concentration profiles at the oxic-anoxic interface: a microsensor study of the hindgut of the wood-feeding lower termite Reticulitermes flavipes (Kollar). Appl. Environ. Microbiol. **63:**4039–4046
16. **Gich, F., J. Garcia-Gil, and J. Overmann.** 2001. Previously unknown and phylogenetically diverse members of the green nonsulfur bacteria are indigenous to freshwater lakes. Arch. Microbiol. **177:**1–10.
17. **Girbal, L., G. von Abendroth, M. Winkler, P. M. Benton, I. Meynial-Salles, C. Croux, J. W. Peters, T. Happe, and P. Soucaille.** 2005. Homologous and heterologous overexpression in *Clostridium acetobutylicum* and characterization of

purified clostridial and algal Fe-only hydrogenases with high specific activities. Appl. Environ. Microbiol. **71:**2777–2781.

18. **Jang, A., J.-H. Lee, P. R. Bhadri, S. A. Kumar, W. Timmons, F. R. Beyette, Jr., I. Papautsky, and P. L. Bishop.** 2005. Miniaturized redox potential probe for in situ environmental monitoring. Environ. Sci. Technol. **39:**6191–6197.

19. **Kane, M. D., L. K. Poulsen, and D. A. Stahl.** 1993. Monitoring the enrichment and isolation of sulfate-reducing bacteria by using oligonucleotide hybridization probes designed from environmentally derived 16S rRNA sequences. Appl. Environ. Microbiol. **59:**682–686.

20. **Lanthier, M., B. Tartakovsky, R. Villemur, G. DeLuca, and S. R. Guiot.** 2002. Microstructure of anaerobic granules bioaugmented with *Desulfitobacterium frappieri* PCP-1. Appl. Environ. Microbiol. **68:**4035–4043.

21. **Lens, P. N., D. de Beer, C. C. Cronenberg, F. P. Houwen, S. P. Ottengraf, and W. H. Verstraete.** 1993. Heterogeneous distribution of microbial activity in methanogenic aggregates: pH and glucose microprofiles. Appl. Environ. Microbiol. **59:**3803–3815.

22. **Liu, W. T., O. C. Chan, and H. H. P. Fang.** 2002. Characterization of microbial community in granular sludge treating brewery wastewater. Water Res. **36:**1767–1775.

23. **Lorenzen, J., L. H. Larsen, T. Kjar, and N. P. Revsbech.** 1998. Biosensor detection of the microscale distribution of nitrate, nitrate assimilation, nitrification, and denitrification in a diatom-inhabited freshwater sediment. Appl. Environ. Microbiol. **64:**3264–3269.

24. **Maidak, B. L., G. L. Olsen, N. Larsen, R. Overbeek, M. J. McCaughey, and C. R. Woese.** 1997. The RDP (Ribosomal Database Project). Nucleic Acids Res.

25:109–110.

25. **Manz, W., R. Amann, W. Ludwig, M. Wagner, and K.-H. Schleifer.** 1992. Phylogenetic oligodeoxynucleotide probes for the major subclasses of *Proteobacteria*: problems and solutions. Syst. Appl. Microbiol. **15:**593–600.
26. **McCarty, P. L., and D. P. Smith.** 1986 Anaerobic wastewater treatment. Environ. Sci. Technol. **20:**1200–1206.
27. **Meier, H., R. Amann, W. Ludwig, and K.-H. Schleifer.** 1999. Specific oligonucleotide probes for *in situ* detection of a major group of gram-positive bacteria with low DNA G+C content. Syst. Appl. Microbiol. **22:**186–196.
28. **Neef, A.** 1997. Anwendung der *in situ*-Einzelzell-Identifizierung von bakterin zur populationsanalyse in komplexen mikrobiellen Biozönosen. Ph.D. thesis. Technische Universität München, Munich, Germany.
29. **Okabe, S., H. Satoh, and Y. Watanabe.** 1999. In situ analysis of nitrifying biofilms as determined by in situ hybridization and the use of microsensors. Appl. Environ. Microbiol. **65:**3182–3191.
30. **Okabe, S., T. Itoh, H. Satoh, and Y. Watanabe.** 1999. Analyses of spatial distributions of sulfate-reducing bacteria and their activity in aerobic wastewater biofilms. Appl. Environ. Microbiol. **65:**5107-5116
31. **Raskin, L., J. M. Stromley, B. E. Rittmann, and D. A. Stahl.** 1994. Group-specific 16S rRNA hybridization probes to describe natural communities of methanogens. Appl. Environ. Microbiol. **60:**1232–1240.
32. **Roller, C., M. Wagner, R. Amann, W. Ludwig, and K.-H. Schleifer.** 1994. In situ probing of gram-positive bacteria with high DNA G+C content using 23S

rRNA-targeted oligonucleotides. Microbiology **140:**2849–2858.

33. **Saitou, N., and M. Nei.** 1987. The neighbor-joining method: a new method for reconstructing phylogenetic trees. Mol. Biol. Evol. **4:**406–425.

34. **Santegoeds, C. M., L. R. Damgaard, G. Hesselink, J. Zopfi, P. Lens, G. Muyzer, and D. de Beer.** 1999. Distribution of sulfate-reducing and methanogenic bacteria in anaerobic aggregates determined by microsensor and molecular analyses. Appl. Environ. Microbiol. **65:**4618–4629.

35. **Sekiguchi, Y., Y. Kamagata, K. Nakamura, A. Ohashi, and H. Harada.** 1999. Fluorescence in situ hybridization using 16S rRNA-targeted oligonucleotides reveals localization of methanogens and selected uncultured bacteria in mesophilic and thermophilic sludge granules. Appl. Environ. Microbiol. **65:**1280–1288.

36. **Sekiguchi, Y., Y. Kamagata, K. Syutubo, A. Ohashi, H. Harada, and K. Nakamura.** 1998. Phylogenetic diversity of mesophilic and thermophilic granular sludges determined by 16S rRNA gene analysis. Microbiology **144:**2655–2665

37. **Thompson, J. D., D. G. Higgins, and T. J. Gibson.** 1994. CLUSTAL W: improving the sensitivity of progressive multiple sequence alignment through sequence weighting, position-specific gap penalties and weight matrix choice. Nucleic Acids Res. **22:**4673–4680.

38. **Voolapalli, R. K., and D. C. Stuckey.** 1999. Relative importance of trophic group concentrations during anaerobic degradation of volatile fatty acids. Appl. Environ. Microbiol. **65:**5009–5016.

39. **Weisburg, W. G., S. M. Barns, D. A. Pelletier, and D. J. Lane.** 1991. 16S ribosomal DNA amplification for phylogenetic study. J. Bacteriol. **173:**697–703.

40. **Whitehead, T. R., and M. A. Cotta.** 1999. Phylogenetic diversity of methanogenic Archaea in swine waste storage pits. FEMS Microbiol. Lett. **179:**223–226.

41. **Yamada, T., Y. Sekiguchi, H. Imachi, Y. Kamagata, A. Ohashi, and H. Harada.** 2005. Diversity, localization, and physiological properties of filamentous microbes belonging to *Chloroflexi* subphylum I in mesophilic and thermophilic methanogenic sludge granules. Appl. Environ. Microbiol. **71:**7493–7503.

42. **Yamaguchi, T., S. Yamazaki, S. Uemura, I. C. Tseng, A. Ohashi, and H. Harada.** 2001. Microbial-ecological significance of sulfide precipitation within anaerobic granular sludge revealed by microsensors study. Water Res. **35:**3411–3417.